

AN IMPROVED AIR-LIGHT ESTIMATION SCHEME FOR SINGLE HAZE IMAGES USING COLOR CONSTANCY PRIOR

Sidharth Gautam , Tapan Kumar Gandhi , B.K. Panigrahi

Indian Institute of Technology, New Delhi

ABSTRACT

Hazy environment attenuates the scene radiance and causes difficulty in distinguishing the color and texture of the scene. A crucial step in dehazing is the recovery of the global air-light vector. Traditional methods usually interpret the RGB value of the brightest region in haze images as the air-light. In this paper, a new prior called 'color constancy prior' has been proposed to improve the robustness of air-light estimation when varicolored illumination exists. The prior utilizes the statistical observation that distant scenery objects become the most haze-opaque due to the pixel escalation towards the higher intensity side. The comparative evaluation on a variety of haze images manifests that the proposed prior perform better than existing air-light recovery methods and can be used for subsequent dehazing applications.

Index Terms— Air-light estimation, dehazing

1. INTRODUCTION

The atmospheric light absorbed and scattered by haze or smoky environment obscure the scene visibility due to the addition of an ambient light layer called air-light. The ambient air-light layer fades the true colors by adding whiteness in the scene and cause a reduction in overall image clarity. Based on this observation, the influences of air-light on natural images can be described using a haze model [1]-[2]:

$$I(\mathbf{x}) = J(\mathbf{x})T(\mathbf{x}) + A_{\infty}(1 - T(\mathbf{x})) \quad (1)$$

$$T(\mathbf{x}) = e^{-\beta d(\mathbf{x})} \quad (2)$$

where I and $J \in \mathbb{R}^{M \times N \times 3}$ are the haze and the haze-free image, $\mathbf{x} = f(x, y) \in \mathbb{R}^2$ is the pixel coordinates, $T \in \mathbb{R}^{M \times N}$ is the transmission-map exponentially related to the scattering coefficient ($\beta \in \mathbb{R} \mid 0 < \beta \leq n$) and scene-depth $d(\mathbf{x}) \in \mathbb{R}^{M \times N}$, $A_{\infty} = [A_{\infty}^r, A_{\infty}^g, A_{\infty}^b] \in \mathbb{R}^3$ is the RGB vector representing the intensity of the air-light. In Eq. (1), air-light contribution, depends on the scattering coefficient (β) and scene-depth $d(\mathbf{x})$ is often defined by the term $A_{\infty}(1 - T(\mathbf{x}))$. In an ideal case, the range of $d(\mathbf{x})$ is $[0, +\infty)$ which makes the pixel values of $T(\mathbf{x})$ lies within the range $0 < T(\mathbf{x}) \leq 1$.

$$I(\mathbf{x}) = J(\mathbf{x}), \quad \text{when } d(\mathbf{x}) \rightarrow 0, \quad T(\mathbf{x}) \rightarrow 1 \quad (3)$$

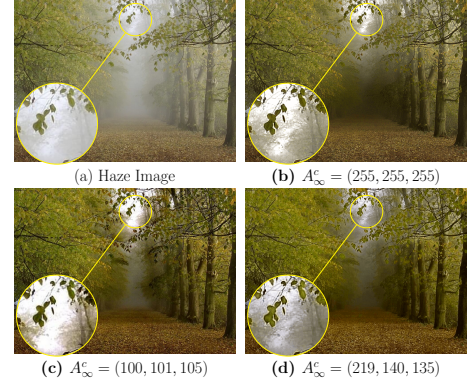


Fig. 1: Significance of estimation of air-light (A_{∞}) in dehazing framework. (a) Real haze image. (b) Over-estimated A_{∞} by He et al. [1], (c) Under-estimated A_{∞} impact by Berman et al. [3] (d) Accurately estimated A_{∞} impact by our method.

Similarly,

$$I(\mathbf{x}) = A_{\infty}, \quad \text{when } d(\mathbf{x}) \rightarrow \infty, \quad T(\mathbf{x}) \rightarrow 0 \quad (4)$$

In terrestrial imaging, Eq. (4) implies that influence of air-light is stronger, when a scenery object exists at very large distance from the camera ($e^{-\beta d(\mathbf{x})} \approx 0$). Likewise, Eq. (3) implies that for shorter distance objects, the observed image is the actual scene radiance. However, in practical situations, both the ideal scenario given by Eq. (3) and Eq. (4) are not possible. Therefore, it becomes essential to investigate both A_{∞} and $T(\mathbf{x})$ independently, to recover the haze-free image $J(\mathbf{x})$. Although, extensive research has been done independently for $T(\mathbf{x})$ estimation, the A_{∞} estimation task is still considered in an ad-hoc manner. The importance of accurate air-light estimation is shown in Fig. 1 where the over-estimation of A_{∞} causes darker dehazing results (see color of tree leaves and pathways in Fig. 1(b)), whereas due to the under-estimation of A_{∞} microscopic details are lost from the bright fields (see Fig. 1(c)). In contrast, an accurate estimation of A_{∞} provides detailed dehazing effects (see Fig. 1(d)).

In earlier dehazing works [4, 5], the brightest pixels value was usually interpreted as the global air-light vector. However, practically in some situations, the brightest pixel may cause extreme failure due to its correspondence towards a gloomy object rather than the air-light. Later, He et al. [1]

solved this ambiguity by choosing the upper 0.1% of brightest pixels among the pixels of the dark channel. Tarel and Hautire *et al.* [6] ignores the existence of true air-light by selecting the pixel value of pure white [255, 255, 255] as the global air-light vector. This method does not recover the ambient light of the scene and often causes global darkness. In contrast, Meng *et al.* [7] uses the upmost pixel value of each RGB channel as the representative of global air-light. Sulami *et al.* [8] takes advantage of the Fattal color-line model [9] for the estimation of air-light magnitude and orientation. However, when distinct colors unable to form a line, the method fails to satisfy the assumption of the color-line model and causes extreme color-shifts. Inspired by color-line model, Berman *et al.* [3] introduced haze-line model. The model is utilizing the observation that pixels after blending with haze form a line pointing towards air-light, and their location could be estimated using the Hough transform in the RGB space. Although the method works well to estimate distinct colors under different depth ranges, it is computationally intensive and often produces an over-exposed region due to the under-estimation of air-light. Bahat and Irani [10] calculates air-light using the patch recurrence property. Zhu *et al.* [11] unites the color-line model and the haze-line model into the color-plane model for air-light estimation. The method uses RANSAC to approximate the air-light orientation and utilizing the global brightness assumption for magnitude estimation. The method is computationally intensive and causes an error when the assumptions are not satisfied.

2. BACKGROUND

In this section, we first describe a technique that is accepted by the majority of the researcher for air-light estimation.

2.1. Dark Channel Prior

The dark channel prior [1] is widely used for global air-light (A_∞) estimation [13, 14, 15]. Mathematically, the dark channel of a hazy input $I(\mathbf{x})$ is defined using:

$$I^{dk}(\mathbf{x}) = \min_{\mathbf{y} \in \Omega(\mathbf{x})} \left(\min_{c \in \{r, g, b\}} I^c(\mathbf{y}) \right) \quad (5)$$

where, I^c is the c^{th} color-channel, Ω is an image local patch centered at pixel \mathbf{x} . By using DCP [1], the air-light (A_∞) contribution can be determined by selecting the upmost 0.1% of brightest pixels in the dark channel as:

$$A_\infty^c = I^c \left(\arg \max_{\mathbf{x} \in P_{0.1\%}} (I^{dk}(\mathbf{x})) \right) \quad (6)$$

In Eq. (6), among 0.1% of brightest pixels, the pixels corresponding to the utmost intensity in c^{th} color-channel of I are selected as the global air-light vector. Moreover, some variants of the air-light (A_∞) estimation modules [2, 7, 8, 16] has been in trend, but a majority of the dehazing works still rely either on DCP [1] or user input.

2.2. Limitations

Despite good performance, the DCP has some limitations:

2.2.1. Over-estimation of air-light (A_∞)

The intensity of the luminous objects such as the lamps and sky is often mistakenly selected as air-light (A_∞), especially when scenery objects brighter than the haze exist. An impact of air-light over-estimation could be easily seen in Fig. 1(b).

2.2.2. Inefficient estimation of transmission-map $T(\mathbf{x})$

On using DCP's Eq. (5) on Eq. (1), $T(\mathbf{x})$ can be derived as:

$$T(\mathbf{x}) = 1 - w \left\{ \min_{\Omega} \left(\min_c \left(\frac{I^c(\mathbf{x})}{A_\infty^c} \right) \right) \right\} \quad (7)$$

In haze, the local-color mixes with the air-light making it difficult to perceive the true colors. In such cases, Eq. (7) yields:

$$\min_{\Omega} \left(\min_c \left(\frac{I^c(\mathbf{x})}{A_\infty^c} \right) \right) \rightarrow 1 \quad \text{and} \quad T(\mathbf{x}) \rightarrow 0 \quad (8)$$

Eq. (8) implies, DCP fails to obtain $T(\mathbf{x})$ when the intensity of any luminous scenery object becomes similar to the A_∞ .

3. PROPOSED METHODOLOGY

In this section, a novel statistical approach based on exploiting the haze impacts in different depth regions of an image is introduced for the air-light estimation.

3.1. Color Constancy Prior

The Color Constancy Prior (i.e., CCP) is based on the statistical observation that deeper-depth regions in an image can be regarded as the most haze-opaque. Although this observation has been widely accepted for $T(\mathbf{x})$ estimation [13]. The novelty of this paper is primarily to use this observation for A_∞ estimation rather than $T(\mathbf{x})$ estimation. Fig. 2 shows an illustration of the haze-statistics. In Fig. 2(b), it can be seen that according to the average histogram plotted for distinct image patches located at different scene-depths, the influence of air-light (i.e., brightness) is pretty low in the regions of shallow-depth and stronger in the regions of deeper-depth. Furthermore, it can also be confirmed from the (A_∞) profile shown in Fig. 2(c) that A_∞ contribution rapidly varies with the scene-depth $d(\mathbf{x})$ and attains a highest value for the distant scenery object. Therefore, inspired by such experimental observation, it can be said that in deeper-depth region, the actual color of the pixel escalates towards the higher intensity side becomes the most haze-opaque and contains a reasonable amount of air-light (A_∞). To describe the A_∞ distribution in haze images, we have named this statistical observation as color constancy prior. Mathematically, the CCP is derived as:

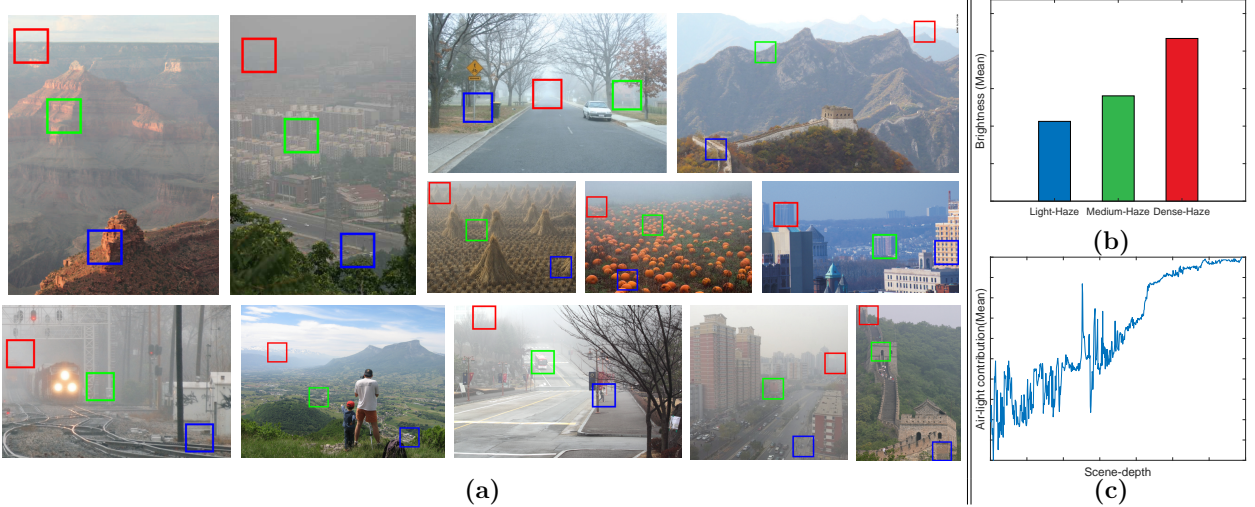


Fig. 2: Pictorial illustrations to represent the haze impacts in different regions of an image. (a) Original haze images with manually identified light-haze, medium-haze, and dense-haze regions [12]. (b) Average histogram of all haze-regions. (c) The air-light profile along the scene-depth (Note: the brightness mean in Fig. 2(b) is generated from 4000 manually extracted 71×71 close-up patches, whereas in Fig. 2(c) the air-light profile is generated from 400 real haze images).

$$h_i = \min_{\mathbf{y} \in \Omega_i(\mathbf{x}_i)} I_{hsv}^v(\mathbf{y}) \quad (9)$$

where "v" is the escalated pixel brightness in the HSV color space. To find A_∞ , first sort the unordered collection of pixel elements in vector $H = \{h_i\}_{i=1}^N$, ($N = M \times N$) in descending order. Since H is a finite length vector after N -steps, we get an ordered sequence of elements S_1 as:

$$S_1 = [h_1^*, h_2^*, h_3^*, \dots, h_N^*] \quad (10)$$

where $h_1^* = \max \{H\}$, $h_N^* = \min \{H\}$. After sorting S_1 , upper $\alpha\%$ of pixels are identified as the brightest pixels (K_B):

$$K_B = I_{hsv}^v(S_1) = \{k_{B1}, k_{B2}, k_{B3}, \dots, k_{BM}\} \quad (11)$$

where $M < N$, $L_1 = \left\{ i \mid h_i \geq h_{\frac{N}{\alpha}}^* \right\}$ is the index of α brightest pixels. Among K_B , there might be few pixels corresponding to the most luminous scenery object, which may cause wrong-estimation of A_∞ . Therefore, to solve this problem, the brightest pixel set (K_B) is sorted in descending order:

$$S_2 = [k_{B1}^*, k_{B2}^*, k_{B3}^*, \dots, k_{BM}^*] \quad (12)$$

where $k_{B1}^* = \max \{K_B\}$, $k_{BM}^* = \min \{K_B\}$. After sorting S_2 , the primary $\gamma\%$ of pixels corresponding to the brightest ones are ignored to identify the brighter pixels (K_b):

$$K_b = I_{hsv}^v(S_2) = \{k_{b1}, k_{b2}, k_{b3}, \dots, k_{bM'}\} \quad (13)$$

where $M' < M$, $L_2 = \left\{ j \mid k_{Bj}^* < k_{B\frac{M}{\gamma}}^* \right\}$ is the index of brighter pixels. Once, we obtained the indices of the brighter pixels, the global air-light vector A_∞ can be estimated using:

$$A_\infty = I \left[\text{mod}(F, M), \lceil \frac{F}{M} \rceil \right] \quad (14)$$

where $F = \min\{L_4\}$, $L_4 = \{L_1(j) \mid j \in L_3\}$, and $L_3 = \{j \mid K_{bj} = \max(K_b)\}$. In the definition of L_4 , the brighter pixel index of L_3 is used for L_1 so that the utmost brighter pixels index can be searched effectively. Among L_4 , there might be many possible indices of the brighter pixel, so the closest index can be chosen using $F = \min\{L_4\}$. In Eq. (14), $\text{mod}(F, M)$ and $\lceil \frac{F}{M} \rceil$ are used to retrieve the location of the most haze-opaque pixels in the input image I .

4. EVALUATION AND RESULTS

This section presents an assessment of the proposed method on a variety of terrestrial [10, 12] and underwater haze images [17], where considerable variation in haze and illumination exists. To validate the performance, a subjective study has been performed on 50 participants using the Bradley-Terry model [18] to manually identify the GT of A_∞ from the most haze-opaque region. After some extensive experiments the parameters are set to $\alpha = 10$ and $\gamma = 0.4$. An example of A_∞ estimation for different types of haze images is shown in Fig. 3. On zooming Fig. 3(b), it can be seen that He et al. [1] and Meng et al. [7] methods often selects the intensity of the brightest region as A_∞ whereas the proposed CCP derives A_∞ from the most haze-opaque regions. Notably, the proposed CCP is intended to retrieve only A_∞ so that it could be used efficiently in Eq. (1) for $J(\mathbf{x})$ retrieval. Therefore, to quantitatively measure the relative error, a classic metric namely mean L2-norm has been used. As can be seen from experimental validation in Fig. 4, the proposed CCP can

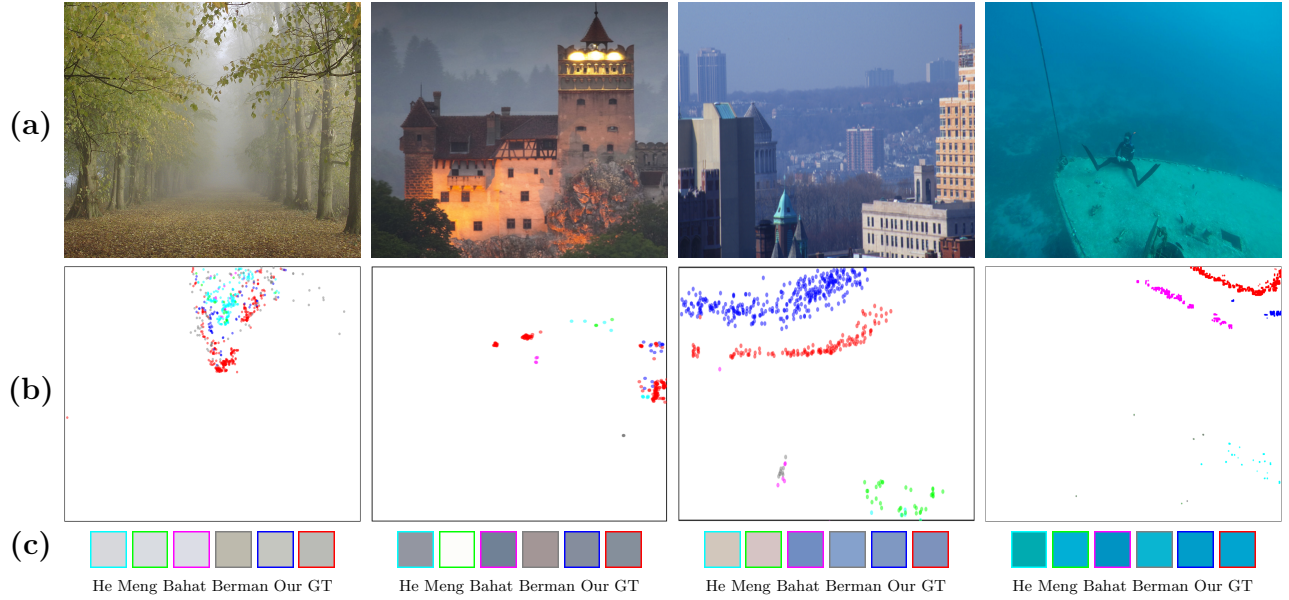


Fig. 3: An example of global air-light (A_∞) estimation with other state-of-the-art methods. (a) Real haze images. (b) The air-light (A_∞) pixel clusters, where each colors corresponds to a different (A_∞) value. (c) The air-light (A_∞) color estimated by He et al. [1], Meng et al. [7], Bahat et al. [10], Berman et al. [3] and ours along with manually identified GT.

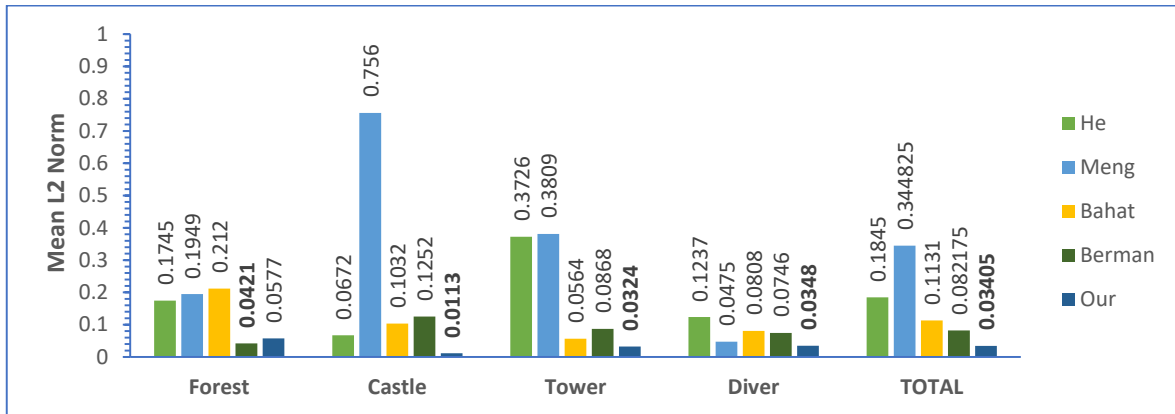


Fig. 4: Accuracy evaluation of global air-light (A_∞) estimation in terms of Mean L2-norm.

Table 1: AVERAGE RUN-TIME (Sec.) COMPARISON.

Image Resolution	He et al. [1]	Meng et al. [7]	Bahat et al. [10]	Berman et al. [3]	Our
(768 × 434)	0.27	0.52	29.51	7.96	0.20
(1024 × 768)	0.58	1.38	53.36	11.81	0.45

consistently estimate A_∞ closer to GT even when luminous scenery objects and unwanted color-cast exist. The run-time comparison using MATLAB R2019a on a PC with Intel® Core™ i7-3770 CPU@ 3.40GHz, 4Core(s), 8GB RAM under 64-bit OS (Microsoft® Windows™ 10 Pro) are summarized in Table-1. The time complexity of the proposed CCP is $O(N)$, compared to [3, 10] which are quadratic.

5. CONCLUSION

In this paper, the problem of air-light estimation in single haze images is addressed and proposed a theoretically well-grounded color constancy prior (CCP) for their retrieval. The CCP is inspired by the statistical observation that in distant scenery objects, the true color of a pixel becomes the most haze-opaque. The CCP is simple, fast, and can easily retrieve the air-light (A_∞) even under considerable variation in illumination. Experimental results on a variety of haze images demonstrate that the proposed CCP is effective and performs better than other state-of-the-art air-light recovery methods. In future work, we intend to examine the performance of CCP on sandstorm images influenced by severe color-cast.

6. REFERENCES

- [1] K. He, J. Sun, and X. Tang, “Single image haze removal using dark channel prior,” *IEEE Transactions on Pattern Analysis and Machine Intelligence*, vol. 33, no. 12, pp. 2341–2353, Dec 2011.
- [2] D. Berman, T. Treibitz, and S. Avidan, “Air-light estimation using haze-lines,” in *2017 IEEE International Conference on Computational Photography (ICCP)*, May 2017, pp. 1–9.
- [3] D. Berman, T. Treibitz, and S. Avidan, “Non-local image dehazing,” in *2016 IEEE Conference on Computer Vision and Pattern Recognition (CVPR)*, June 2016, pp. 1674–1682.
- [4] R. T. Tan, “Visibility in bad weather from a single image,” in *2008 IEEE Conference on Computer Vision and Pattern Recognition*, June 2008, pp. 1–8.
- [5] Raanan Fattal, “Single image dehazing,” *ACM Trans. Graph.*, vol. 27, no. 3, pp. 1–9, Aug. 2008.
- [6] Jean-Philippe Tarel and Nicolas Hautière, “Fast visibility restoration from a single color or gray level image,” in *Proceedings of IEEE International Conference on Computer Vision (ICCV’09)*, Kyoto, Japan, 2009, pp. 2201–2208, <http://perso.lcpc.fr/tarel.jean-philippe/publis/iccv09.html>.
- [7] G. Meng, Y. Wang, J. Duan, S. Xiang, and C. Pan, “Efficient image dehazing with boundary constraint and contextual regularization,” in *2013 IEEE International Conference on Computer Vision*, Dec 2013, pp. 617–624.
- [8] M. Sulami, I. Glatzer, R. Fattal, and M. Werman, “Automatic recovery of the atmospheric light in hazy images,” in *2014 IEEE International Conference on Computational Photography (ICCP)*, May 2014, pp. 1–11.
- [9] Raanan Fattal, “Dehazing using color-lines,” *ACM Trans. Graph.*, vol. 34, no. 1, pp. 13:1–13:14, Dec. 2014.
- [10] Y. Bahat and M. Irani, “Blind dehazing using internal patch recurrence,” in *2016 IEEE International Conference on Computational Photography (ICCP)*, May 2016, pp. 1–9.
- [11] Mingzhu Zhu, Bingwei He, and Liwei Zhang, “Atmospheric light estimation in hazy images based on color-plane model,” *Computer Vision and Image Understanding*, vol. 165, 10 2017.
- [12] L. K. Choi, J. You, and A. C. Bovik, “Referenceless prediction of perceptual fog density and perceptual image defogging,” *IEEE Transactions on Image Processing*, vol. 24, no. 11, pp. 3888–3901, 2015.
- [13] Q. Zhu, J. Mai, and L. Shao, “A fast single image haze removal algorithm using color attenuation prior,” *IEEE Transactions on Image Processing*, vol. 24, no. 11, pp. 3522–3533, Nov 2015.
- [14] B. Cai, X. Xu, K. Jia, C. Qing, and D. Tao, “Dehazenet: An end-to-end system for single image haze removal,” *IEEE Transactions on Image Processing*, vol. 25, no. 11, pp. 5187–5198, Nov 2016.
- [15] Dong Yang and Jian Sun, “Proximal dehaze-net: A prior learning-based deep network for single image dehazing,” in *ECCV*, 2018.
- [16] Ming-Zhu Zhu, Bing-Wei He, and Li-Wei Zhang, “Atmospheric light estimation in hazy images based on color-plane model,” *Computer Vision and Image Understanding*, vol. 165, pp. 33 – 42, 2017.
- [17] C. Li, C. Guo, W. Ren, R. Cong, J. Hou, S. Kwong, and D. Tao, “An underwater image enhancement benchmark dataset and beyond,” *IEEE Transactions on Image Processing*, vol. 29, pp. 4376–4389, 2020.
- [18] Otto Dykstra, “Rank analysis of incomplete block designs: A method of paired comparisons employing unequal repetitions on pairs,” *Biometrics*, vol. 16, no. 2, pp. 176–188, 1960.